DEVELOPMENT OF A 5-COMPONENT BALANCE FOR WATER TUNNEL APPLICATIONS*

Carlos J. Suárez, Brian R. Kramer and Brooke C. Smith
EIDETICS CORPORATION

SUMMARY

The principal objective of this research/development effort was to develop a multi-component strain gage balance to measure both static and dynamic forces and moments on models tested in flow visualization water tunnels. A balance was designed that allows measuring normal and side forces, and pitching, yawing and rolling moments (no axial force). The balance mounts internally in the model and is used in a manner typical of wind tunnel balances. The key differences between a water tunnel balance and a wind tunnel balance are the requirement for very high sensitivity since the loads are very low (typical normal force is 90 grams or 0.2 lbs), the need for water proofing the gage elements, and the small size required to fit into typical water tunnel models. The five-component balance was calibrated and demonstrated linearity in the responses of the primary components to applied loads, very low interactions between the sections and no hysteresis. Static experiments were conducted in the Eidetics water tunnel with delta wings and F/A-18 models. The data were compared to forces and moments from wind tunnel tests of the same or similar configurations. The comparison showed very good agreement, providing confidence that loads can be measured accurately in the water tunnel with a relatively simple multi-component internal balance. The success of the static experiments encouraged the use of the balance for dynamic experiments. Among the advantages of conducting dynamic tests in a water tunnel are less demanding motion and data acquisition rates than in a wind tunnel test (because of the low-speed flow) and the capability of performing flow visualization and force/moment (F/M) measurements simultaneously with relative simplicity. This capability of simultaneous flow visualization and for F/M measurements proved extremely useful to explain the results obtained during these dynamic tests. In general, the development of this balance should encourage the use of water tunnels for a wider range of quantitative and qualitative experiments, especially during the preliminary phase of aircraft design.

NOMENCLATURE

YM_1	Yawing moment section #1	YM_2	Yawing moment section #2
PM_1	Pitching moment section #1	PM_2	Pitching moment section #2
RM	Rolling moment section	Co	Root chord
$\bar{c}$	Mean aerodynamic chord	b	Wing Span
α	Angle of attack, deg	α_0	Mean angle of attack, deg
β	Sideslip angle, deg	ϕ	Roll angle, deg
Q_∞	Free stream dynamic pressure	V_∞	Free stream velocity
M	Mach number	Re	Reynolds number
C_N	Normal force coefficient	f	Oscillation frequency, Hz
C_m	Pitching moment coefficient (body axis)	a	Acceleration, deg/sec^2

* Work done at EIDETICS under SBIR Contract NAS2-13571

C_Y	Side force coefficient (body axis)	q	Pitch rate, deg/sec
C_n	Yawing moment coefficient (body axis)	ω	Angular velocity, deg/sec
C_l	Rolling moment coefficient (body axis)	k	Reduced frequency, $\frac{\pi f \bar{c}}{V_\infty}$
ω_{max}	Max. angular velocity, deg/sec	q_o	Non-dim. pitch rate, $\frac{q \bar{c}}{2 V_\infty}$
Ω	Non-dimensional rotation rate, $\frac{\omega\,[rad/sec]\,b}{2 V_\infty}$		

INTRODUCTION

Water tunnels have been utilized in one form or another to explore fluid mechanics and aerodynamics phenomena since the days of Leonardo da Vinci. Many studies (Refs. 1-6) have shown that the flow fields and the hydrodynamic forces in water tunnels are equivalent to the aerodynamic flow fields and forces for models in wind tunnels for the incompressible flow regime (i.e., Mach numbers less than 0.3). Only in recent years, however, have water tunnels been recognized as highly useful facilities for critical evaluation of complex flow fields on many modern vehicles such as high performance aircraft. In particular, water tunnels have filled a unique role as research facilities for understanding the complex flows dominated by vortices and vortex interactions. Flow visualization in water tunnels provides an excellent means for detailed observation of the flow around a wide variety of configurations. The free stream flow and the flow field dynamics are low-speed, allowing real-time visual assessment of the flow patterns using a number of techniques including dye injection, hydrogen bubbles, laser sheet illumination, etc.

Water tunnel testing is attractive because of the relatively low cost and quick turn-around time to perform experiments and evaluate the results. Models are relatively inexpensive (compared to wind tunnel models) and can be built and modified as needed in a relatively short time period. The response of the flow field to changes in model geometry can be directly assessed in water tunnel experiments with flow visualization. One of the principal limitations of a water tunnel, however, is that the low flow speed, which provides for detailed visualization, also results in very small hydrodynamic (aerodynamic) forces on the model, which, in the past, have proven to be difficult to measure accurately. In most cases where force and moment information is essential, wind tunnel tests (usually with a different model) eventually have to be performed. The advent of semi-conductor strain gage technology and devices associated with data acquisition such as low-noise amplifiers, electronic filters, and digital recording has made accurate measurements of very low strain levels feasible. The development of a system to measure the small forces and moments generated in a water tunnel would increase the usefulness of this type of research facility significantly. If the water tunnel could determine forces and moments to some level of accuracy simultaneously with the flow visualization, the interpretation of results would be greatly simplified. Also, it would be possible to quantify the changes produced by configuration modifications, conventional and unconventional control techniques, etc.

In addition to static F/M measurements, the water tunnel balance can also provide a capability for dynamic experiments. The high flow speed typical of wind tunnel tests requires rapid movement of the model in order to simulate a properly scaled dynamic maneuver and the motions are mechanically difficult to implement. The fast model movement also places demanding requirements on the response of the data acquisition system to acquire data at high sample rates. In contrast, the flow speed of water tunnel tests is typically much lower (2 orders of magnitude or more), and consequently, the model motion required to simulate a dynamic maneuver is also very slow. Thus, the response rates for data acquisition required for force and moment measurements during transient and dynamic situations are less demanding than in a wind tunnel.

The specific technical objectives of this research/development project are listed below:

1) Design and fabricate a five-component balance to measure forces and moments in a water tunnel.

2) Calibrate the balance and determine component sensitivities and interactions, i.e., determine the calibration output matrix.

3) Perform static and dynamic experiments on delta wings and F/A-18 models, and compare the results with available wind tunnel or numerical data to assess the performance of the balance.

BALANCE DESCRIPTION

Mechanical Design

Basically, the balance is similar to the sting balances used in wind tunnel tests and is located inside the model (Fig. 1). It consists of a rolling moment section, two pitching moment sections and two yawing moment sections, all 1.91 cm (3/4") in diameter. Five components will provide for the simultaneous measurement of pitching, yawing and rolling moments and normal and side forces. The moment of inertia of each section was carefully calculated in order to obtain the required stress levels that produce the desired sensitivity and resolution when the balance is loaded in the plane of interest and maximum stiffness in the other planes. Each component is attached to the next by means of two screws, and two location pins ensure the perfect alignment between components.

Strain Gages

Semi-conductor strain gages are used to get the desired output, since they are widely acknowledged as being outstanding transduction devices. The change in resistance per unit applied strain results in an output of 50 to 100 times that of either wire or foil strain gages. The gages used have a resistance of 1000 Ω and a gage factor (GF) of 145. They are very small in size, only 0.08 cm (0.03") wide by 0.4 cm (0.16") long. Each section is composed of four gages, connected using a full Wheatstone bridge and of some standard resistors added externally. These resistors are used to compensate for differences in the strain gage resistance and to compensate for temperature changes. The values of the resistors vary for each of the sections and are specified by the gaging company after extensive tests. Temperature compensation for this application is not very critical since the temperature changes during a typical water tunnel test are almost negligible. A 100 Ω potentiometer is used to balance each bridge externally when the internal potentiometer of the signal conditioner is not enough to produce a zero reading under specific loading conditions.

Water Proofing

The fact that the balance has to operate under water complicates the problem significantly, and different water proofing techniques had to be tested until the optimum was found. After the gages, terminals and wires were in place, a layer of silicon rubber was applied over the entire area

where the gages and terminals are located. The balance was later coated with Parylene™, a thin plastic film applied in a vacuum chamber. A rubber sleeve was utilized as a tertiary protection, as seen in Fig. 1.

DATA ACQUISITION/REDUCTION SYSTEM

A multi-channel system was used to provide excitation voltage (5 Volts) to the bridges, and to amplify and condition the output signals. The output lines for each channel were routed both to the digital display of the signal conditioner and to an analog-to-digital (A/D) board inside a Macintosh Quadra 700 computer.

The data acquisition/reduction software was developed specifically for this application using National Instrument's LabView, a graphical programming language. The software provides an interface that is user friendly and is versatile in its ability to reduce and display the balance and tunnel condition data efficiently. The basic methodology for the data reduction system, particularly the treatment of the balance equations, is based on the same approach used for typical wind tunnel data reduction schemes. The data acquisition/reduction software allows to perform a full balance calibration, as well as to acquire and reduce data during static and dynamic experiments. It allows the user to display "on-line" signals, acquire data at specified sampling rates and to reduce the data to coefficient form. Files with raw and coefficient data are created and saved to a disk for later plotting or reprocessing.

BALANCE CALIBRATION

A key to accurately acquiring data from an internal balance is a precise and repeatable calibration. For a multi-component balance, it is important to determine the response of each section to a load in its primary plane of action (sensitivity) and also to loads in other planes (interactions). For example, the output from a pitching moment gage will depend not only on the direct application of a pitching moment (or a normal force) but will also respond to a rolling moment or a yawing moment input. The objective is to minimize these interactive load/response characteristics, but the expense of manufacturing a balance to the tolerance levels to approach zero interactions is not warranted since the interactions can now be accounted for quite easily on modern computers. Therefore, appropriate calibration hardware, software and procedures are essential to obtain the correct sensitivities and interactions.

Calibration Rig

A simple calibration apparatus, shown in Fig. 2, was designed and built to calibrate the five-component balance. Basically, the rig consist of a main aluminum support where the sting mount and balance are attached. Pulleys on each side of the balance can be used to obtain accurate side forces and rolling moments. The pulley system permits the application of a pure rolling moment provided that low friction pulleys are used and the cables are perfectly aligned. Each pulley is mounted on a shaft between two bases that slide along a side rail. The bases can also be moved up and down, so the pulley can be accurately positioned to obtain the desired load. A loading fixture attached to the balance end is used to apply the weights at the desired load points. The loading fixture can be rotated to get the proper configuration according to the desired type of loading. The balance can also be rotated; therefore, the required loading can be obtained either by

rotating the balance or the loading fixture. Levels and stainless steel pins ensure the perfect alignment of the balance and the rig throughout the calibration process.

Calibration Results

A full calibration was performed using the calibration rig and standard procedures typical of wind tunnel sting balances. The balance was loaded at five load points with positive and negative normal and side forces, and at the balance reference center (Load Point 3, LP3) with positive and negative rolling moments. The software developed acquires and graphs the data for the different loading cases, applying a linear curve fit. After all the graphs are created, it automatically builds the calibration input matrix. By inverting the input matrix, the calibration output matrix is obtained. This matrix allows to obtain engineering units from the voltages at each section, applying all the correct sensitivities and interactions.

Figure 3 presents an example of a loading case, i.e., the response of the five channels to a normal force applied at LP4. As expected, the largest response is seen in Channel 1 (CH1), which corresponds to the most forward pitching moment section. Since the load is applied exactly at the location of the second pitching moment section (CH3), this channel does not react to this particular loading. Interactions with the rolling moment and yawing moment sections (CH0, CH2, CH4) are very small.

After all the loading cases were completed, the slopes of the output of each channel at the different load points were plotted versus the distance to said load points. Figure 4 shows one of these plots, in this case, the response of the pitching moment gauges to an applied pitching moment. The slopes of the lines (approximately 0.009 Volts/in-lb) are the sensitivity to pitching moment, while the y-intercepts are the sensitivity of these channels to a normal force. Figure 5 presents, in a similar manner, the sensitivity of the yawing moment gages to an applied yawing moment (0.026 Volts/in-lb).

The rolling moment calibration is presented in Fig. 6. Pure positive and negative rolling moments were applied at LP3, and the output at the gages in Volts is plotted versus moment for the five channels. The response of the rolling moment component (CH2) is linear, both for the positive and negative cases. The slope of this line represents the sensitivity of the section to rolling moment, i.e., -0.0097 Volts/in-lb (average of the slopes of the positive and negative loading cases). Interactions with the other sections are negligible.

Hysteresis was also investigated to complete the calibration. The balance was loaded and then unloaded using the same weight increments. All possible loading cases were investigated, i.e., positive and negative side and normal forces, and positive and negative rolling moments. The balance showed no hysteresis on any of the channels under primary loads.

EXPERIMENTAL SETUP

Water Tunnel

All experiments were conducted in the Eidetics Model 2436 Flow Visualization Water Tunnel. The facility is a continuous horizontal flow tunnel with a test section 0.91 m (3 ft) high x 0.61 m (2 ft) wide x 1.83 m (6 ft) long. The model is mounted inverted, and it is possible to test at angles of attack between 0° and 65°, and at sideslip angles between -25° and 25°.

Models

A 70° flat plate delta wing and F/A-18 models were used for these experiments. The aluminum delta wing (Fig. 7) has a root chord of 15 inches and a double-beveled leading edge. The balance is located at the model centerline and two fiberglass fairings (top and bottom) covered the entire balance. The 1/32nd-scale F/A-18 model is shown in Fig. 8. The reason for choosing the F/A-18 was the availability of data from several wind tunnel tests on this configuration that could be used for direct comparison to evaluate the performance of the balance. The plastic model is equipped with dye ports for flow visualization and the balance is attached to an internal aluminum plate. Control surfaces were fixed at 0° throughout the entire test (leading edge flaps were fixed at 34°). The rotary balance experiments were performed on a 1/48th-scale F/A-18 due to size constraints in the water tunnel. The width of the test section (24 inches) did not allow the use of the 1/32nd-scale F/A-18 model utilized for the other dynamic experiments. The smaller plastic model has a span of 10 inches and a total length of 14 inches. Moments are referenced to the 50% $\bar{c}$ on the delta wing and to the 25% $\bar{c}$ on the F/A-18 models, except when indicated.

STATIC WATER TUNNEL EXPERIMENTS

Methodology And Boundary Corrections

The static tests were performed following standard "wind tunnel procedures". The gages were zeroed at the beginning of each run with the model at $\alpha = \beta = \phi = 0°$. A static tare (or weight tare) was performed before the actual run. This consists of an angle of attack sweep with the tunnel off ($Q_\infty = 0$) to account for gravity effects. After that, the model is always returned to $\alpha = 0°$, a zero point is taken and the tunnel is started.

The water tunnel data were corrected only at high angles of attack. This correction is required as a result of a significant expansion of the wake when the wing stalls and it was developed by Cunningham (Ref. 5). It is a semi-empirical relationship based only on planform blockage and angle of attack. Equations in Ref. 5 are given only for C_N; however, since this is actually a Q_∞ correction, it was also applied to the other components in a similar manner. The correction is applied starting at $\alpha = 38°$ for the delta wings and at $\alpha = 40°$ for the F/A-18 (approximate stall angles for each configuration). Figure 9 shows uncorrected and corrected data for the 70° delta wing at zero sideslip, with the largest changes occurring in the normal and side forces.

Examples of Static Test Results

Most of the static experiments were conducted at velocities ranging from 12.7 cm/sec (0.42 ft/sec) to 17.8 cm/sec (0.58 ft/sec). This range of velocities corresponds to Reynolds numbers from 34,000 to 47,000 per foot. Data were acquired at 100 samples/sec for 25 seconds and were not filtered. The large number of samples acquired permitted to obtain a mean value that represents the average gage reading at that particular loading condition.

The longitudinal characteristics of the 70° delta wing during static conditions are presented and compared to wind tunnel data in Fig. 10. The water tunnel data (obtained at $V_\infty = 0.58$ ft/sec) are compared to similar data obtained in another water tunnel (Ref. 5), and in the KU 3x4' wind tunnel (Ref. 7), the WSU 7x10' wind tunnel (Ref. 8) and the Langley 12' wind tunnel (Ref. 9). The normal force coefficient agrees very well with most of the data, except for the Langley data. The differences between these data and the other wind tunnel data are quite significant and are probably due to the type of corrections applied, mounting system, flow quality, etc. Since the software provided the moments referenced to the 50% $\bar{c}$, the appropriate transformations had to be applied to obtain C_m at other locations. The pitching moment at 30% $\bar{c}$ is compared to two sets of wind tunnel data and the agreement is satisfactory.

Figure 11 shows a comparison between the water tunnel test and other wind tunnel tests for the baseline F/A-18. Angle of attack sweeps at $\beta = 0°$ were performed and the agreement in C_N is very good, both in slope and absolute magnitude. The data obtained in the water tunnel match not only other small-scale wind tunnel tests (Refs. 10-12), but the full-scale test at the NASA Ames 80x120' (Ref. 13) and the F/A-18 Aero Model used in simulation as well. Only one data set (Langley 12', Ref. 12) has much lower values than those obtained in this test. The pitching moment measurements also agree well with other data; small differences are seen between 45° and 55° angle of attack, but trends and slopes are very similar. Lateral/directional characteristics were compared to data from Ref. 11, as seen in Fig. 12, and similarities in the C_Y and C_l curves during β sweeps at $\alpha = 30°$ are evident. It should be noted that corrections due to wall proximity during sideslip sweeps were not introduced in the data reduction scheme, and therefore, small discrepancies can be expected. These comparisons show that the balance can be used effectively to measure five components of the forces and moments experienced by a "real" configuration (as opposed to "generic", as in the case of the delta wing) in this flow regime. For more information and examples on water tunnel static tests, please see References 14 and 15.

DYNAMIC WATER TUNNEL EXPERIMENTS

Methodology And Boundary Corrections

The motion rates selected for the dynamic tests conducted in the water tunnel should, of course, be scaled properly to represent the correct relationship between rotation rate, scale, and free stream velocity. During the dynamic experiments, the data are corrected at high angles of attack with the same technique utilized during the static water tunnel experiments (Refs. 5, 14 and 15). A weight tare ($V_\infty = 0$) is performed to account for gravity effects as in the static tests. The software handles the entire data acquisition and reduction processes, as well as the model motion. In order to correlate the F/M measurements with the model position, the software takes an encoder reading, then acquires the balance data, takes a second encoder reading and assigns the balance values to the average of the two encoder readings. The number of balance samples acquired between each encoder reading can be varied, and the final value for each channel is the arithmetic average of the samples taken. As expected, the larger the number of samples acquired, the better the quality of the data. It was found that by acquiring 800/1,000 per channel, the data obtained are very smooth and repeatable, requiring no post-processing or curve-fitting and clearly indicating the value of the force/moment at the particular model location. Since the A/D board used allows acquiring data very fast (10,000 samples per second), it was possible to take a large number of samples per channel and still obtain an adequate density of points (again, the low motion rates required in the water tunnel facilitate these experiments). For the rotary balance tests, data were acquired and

averaged over two revolutions to avoid excessive twisting of the cables (no slip-ring was used). A weight tare ($V_\infty = 0$), also averaged over exactly two revolutions, was performed at each angle of attack and subtracted from the "tunnel on" data.

Effect Of Inertial Tares

One of the unknowns in dynamic water tunnel experiments was the model inertia effects on the data, i.e., the effect of the resistance to motion due to the model mass moment of inertia. Before actually performing the experiments, it was calculated that the inertia contribution to the aerodynamic values to be measured would be small, because of the low motion rates used in the water tunnel. The inertia effects are determined by measuring the time-variant moment recorded by the balance with the model in motion with the tunnel velocity at zero. This motion must be identical to the motion generated with the tunnel on ($V_\infty > 0$). The aerodynamic contribution is determined by subtracting the measured moment at $V_\infty = 0$ from the moment measured at $V_\infty > 0$.

Results indicate that the inertial contribution is, indeed, very small. Figure 13a shows the measured normal force on the 70° delta wing during a ramp-hold maneuver from 15° to 60° angle of attack. The value of the normal force N (lbs) measured during the pitch-up motion when the water tunnel is off ($V_\infty = 0$) is almost negligible, approximately 1% of the value measured with tunnel speed. Also included in Fig. 13a is the value of the normal force measured during the specified motion with no water in the tunnel. The value of N throughout the dynamic maneuver under the "no water" condition is very similar to the $V_\infty = 0$ case, indicating that there are no major "virtual mass effects" (resistance of the surrounding water to being displaced by the moving model). Similar results were obtained during pitch oscillations with the F/A-18 models (Fig. 13b), and during the other dynamic experiments (yaw and roll oscillations, rotary balance tests). Therefore, depending on the quality of the data required, the inertia effects can be ignored, facilitating the testing and the data reduction process.

Examples of Dynamic Test Results

Pitch Oscillations (70° Delta Wing Model)

The first set of dynamic experiments consisted of large-amplitude pitch oscillations about a mean angle of attack α_0. The purpose of these tests was to directly compare the water tunnel data to results from wind tunnel tests conducted at NASA Langley by Brandon and Shaw, where a 70° wing was investigated for forces and moments produced by these large-amplitude pitch motions (Ref. 16). Figure 14 presents changes in the normal force coefficient produced by oscillating the delta wing ±18° about different α_0's with a reduced frequency $k = 0.0376$. This k value corresponds to a maximum full-scale pitch rate of approximately 60 deg/sec for a typical fighter aircraft at altitude and at $V_\infty = 200$ ft/sec. The hysteresis loops are evident in the force measurements, with all the cases producing similar values of C_N overshoot. Results from the wind tunnel tests in Ref. 16 are shown in the same figure and the similarities in the two data sets can be clearly identified. The level of C_N is slightly lower in the wind tunnel test, especially above 25°, but the shape of the dynamic loops and the relative increments are very similar in both tests.

Pitch-Up/Down And Hold Maneuvers (F/A-18 Model)

Experiments on the 1/32nd-scale F/A-18 model included pitch-up/down and hold maneuvers. The model rotates about the 25% $\bar{c}$, and the motions are basically constant rate ramps. Figure 15 presents results for pitch-up and hold motions from 15° to 65° angle of attack for different non-dimensional pitch rates q_0. The normal force and pitching moment data show a dependency on pitch rate, as reported by Brandon and Shaw in Ref. 17. This set of experiments was completed with pitch-down and hold maneuvers at different rates. The maneuver consisted of pitching down the F/A-18 model from 65° to 15° angle of attack. The motion profiles for the pitch-up and hold maneuvers, along with the variation of the normal force coefficient with time, are illustrated in Fig. 16. The "persistence" in normal force, defined as the time it takes the force to reach its steady or static value from the moment the motion stopped, is clearly observed. Figure 17 shows the motion profiles and the change in the normal force coefficient versus time for the pitch-down and hold maneuver. It is very interesting to notice that, contrary to the behavior observed during the pitch-up maneuvers in terms of persistence, by the time the model stops after the pitch-down, the value of the normal force is almost the same as the static value, denoting a very small or almost zero persistence. The persistence in C_N, in terms of convective time units, is compared to data from the wind tunnel experiments (Ref. 17) in Fig. 18. A convective time unit is the time it takes one particle in the free stream to travel a distance equal to the mean aerodynamic chord on the model. The similarities between the results from the two experiments are quite evident, indicating similar flows and dynamic force/moment responses.

Rotary-Balance Experiments (F/A-18 Model)

Another important maneuver for present and future aircraft is the "loaded roll" or rolling around the velocity vector at medium to high angles of attack. In the wind tunnel, rotary-balances are used to acquire force and moment data from an internal balance with the model rotating around the velocity vector at varying rotation rates. With the balance, the water tunnel can provide a simplified version of the same type of test capability with the added benefit of being able to observe the behavior of the flow at the same time. The rig consists of an aluminum C-strut that attaches to the roll mechanism and the water tunnel main C-strut (Fig. 19). The angle of attack is changed manually by sliding the arm along the C-strut, allowing testing at angles of attack between 0° and 60°. Once the desired α is obtained, the arm is fixed in position. Sideslip can be varied by rotating the sting in the adapter located at the end of the arm.

As in the other dynamic experiments, it was found that the inertial effects on the data were negligible, and thus, the rotary tare can be performed at any rotation speed. These particular rotary-balance experiments were performed for non-rotational rates Ω up to ± 0.15 and the rotary tares were always conducted at rates corresponding to $\Omega = 0.10$. Data from the water tunnel rotary-balance tests correspond to runs at 0.42 ft/sec and 0.58 ft/sec (Reynolds number of 8,200 and 11,500, respectively). These data are compared to results from a rotary-balance test performed by Eidetics on a 6%-scale F/A-18 in the NASA Ames 7x10' wind tunnel (Ref. 18), and from a test of a 1/10-scale F-18 model at the Langley Spin Tunnel (Ref. 19). Results of F/M measurement at $\alpha = 50°$, presented in Fig. 20, reveal that the normal force coefficient has a similar behavior in all the tests, i.e., a slight increase with rotation rate. The agreement in the lateral/directional coefficients is quite acceptable. Evidently, the forebody vortex flow fields in the water and wind tunnel experiments present opposite asymmetries, as indicated by the side force value at $\Omega = 0$, but the anti-spin slope is similar in both tests. The yawing moment coefficient obtained in the water tunnel presents a smaller slope than that revealed by the wind tunnel results, especially for negative

rotations, denoting again a possible slight shift in the center of pressure. The anti-spin behavior, however, is still present. For more information and examples of water tunnel dynamic experiments, see Ref. 20.

CONCLUSIONS

A five-component balance was designed, built and tested in the Eidetics' water tunnel. The balance was calibrated and showed good linearity and low interactions. Results of static experiments were quite satisfactory, showing good correlation with wind tunnel data of similar configurations (delta wings and F/A-18 models). This research/development project also explored the use of the balance to perform dynamic experiments in the water tunnel. Among the advantages of conducting dynamic tests in a water tunnel are less demanding motion and data acquisition rates than in a wind tunnel test (because of the low-speed flow) and the capability of performing flow visualization and force/moment measurements simultaneously with relative simplicity. Dynamic experiments included pitch, yaw and roll oscillations, pitch-up/down and hold maneuvers and rotary-balance tests. Results obtained in these tests also compared well with wind tunnel data.

In general, results obtained in this research/development project show conclusively that water tunnels can be used effectively for quantitative and qualitative measurements and emphasizes the importance of having the capability of performing simultaneous flow visualization and F/M measurements.

ACKNOWLEDGMENTS

This study was partially supported by NASA Dryden Flight Research Center under SBIR Phase II Contract No. NAS2-13571. The technical monitor was Mr. John Del Frate.

REFERENCES

1. Erickson, G. E., Peake, D. J., Del Frate, J., Skow, A. M., and Malcolm, G. N., "Water Facilities in Retrospect and Prospect - an Illuminating Tool for Vehicle Design", NASA TM 89409, November 1986.

2. Deane J. R., "Wind and Water Tunnel Investigations of the Interaction of Body Vortices and the Wing Panels of a Missile Configuration," AGARD CP-2467, Jan. 1979.

3. Thompson, D. H., "A Water Tunnel Study of Vortex Breakdown Over Wings with Highly Swept Leading Edges," ARL/A-Note-356, Melbourne, May 1975.

4. Davies, A. G., "A Comparative Study of Vortex Flows in Wind and Water Tunnels", presented at the AGARD Fluid Dynamics Panel Symposium on Aerodynamic and Related Hydrodynamic Studies Using Water Facilities, October 1986.

5. Cunningham, A., "Steady and Unsteady Force Testing of Fighter Aircraft Models in a Water Tunnel," AIAA-90-2815, presented at the AIAA 8th Applied Aerodynamics Conference, Portland, Oregon, Aug. 20-22,1990.

6. Malcolm, G.N., Nelson, R.C., "Comparison of Water and Wind Tunnel Flow Visualization Results on a Generic Fighter Configuration at High Angles of Attack," AIAA Paper

87-2423, presented at the AIAA Atmospheric Flight Mechanics Conference, Monterey, CA, Aug. 1987.

7. Wentz, W. H. Jr., "Wind Tunnel Investigations of Vortex Breakdown on Slender Sharp-Edged Wings", Ph.D. Dissertation, University of Kansas, Lawrence, KS.

8. Phillis, D.L., "Force and Pressure Measurements Over a 70° Delta Wing at High Angles of Attack and Sideslip," Master Thesis, Aeronautical Engineering Department, The Wichita State University, 1991.

9. Brandon, J. M. and Shah, G. H., "Effect of Large Amplitude Pitching Motions on the Unsteady Aerodynamic Characteristics of Flat-Plate Wings", AIAA Paper No. 88-4331, presented at the Atmospheric Flight Mechanics Conference, August 15-17, 1988.

10. Kramer, B. R., Suárez, C. J., Malcolm, G. N. and Ayers, Bert F., "F/A-18 Forebody Vortex Control", Eidetics TR-93-003, Volume I (Static Tests), April 1993.

11. Erickson. G. E., Hall, R. M, et. al., "Experimental Investigation of the F/A-18 Vortex Flows at Subsonic Through Transonic Speeds", AIAA Paper 89-2222 (invited), presented at the AIAA 7th Applied Aerodynamics Conference, Seattle, WA, 1989.

12. Brandon, J. M. and Shah, G. H., "Unsteady Aerodynamic Characteristics of a Fighter Model Undergoing Large-Amplitude Pitching Motions at High Angles of Attack", AIAA Paper No. 90-0309, 28th Aerospace Sciences Meeting, January, 1990, Reno, Nevada.

13. Lanser, W. R., Murri, D. G., "Wind Tunnel Measurements on a Full-Scale F/A-18 With Forebody Slot Blowing or Forebody Strakes", AIAA Paper 93-1018, presented at the AIAA/AHS/ASEE Aerospace Design Conference, Irvine, CA, 1993.

14. Suárez, C.J., Ayers, B.F., and Malcolm, G.N., "Force and Moment Measurements in a Flow Visualization Water Tunnel", AIAA 94-0673, presented at the AIAA 32nd Aerospace Sciences Meeting, Reno, Nevada, Jan. 1994.

15. Suárez, C.J. and Malcolm, G.N., "Water Tunnel Force and Moment Measurements on an F/A-18", AIAA 94-1802, presented at the AIAA 12th Applied Aerodynamics Conference, Colorado Springs, CO, June 1994.

16. Brandon, J.M. and Shah, G.H., "Effect of Large Amplitude Pitching Motions on the Unsteady Aerodynamic Characteristics of Flat-Plate Wings," AIAA Paper 88-4331, presented at the Atmospheric Flight Mechanics Conference, August 15-17, 1988.

17. Brandon, J.M. and Shah, G.H., "Unsteady Aerodynamic Characteristics of a Fighter Model Undergoing Large-Amplitude Pitching Motions at High Angles of Attack", AIAA Paper No. 90-0309, 28th Aerospace Sciences Meeting, January, 1990, Reno, Nevada.

18. Kramer, B.R., Suárez, C.J., Malcolm, G.N. and James, K.D., "Forebody Vortex Control on an F/A-18 in a Rotary Flow Field," AIAA Paper 94-0619, presented at the 32nd Aerospace Sciences Meeting, Reno, NV, 1994.

19. Hultberg, R., "Low Speed Rotary Aerodynamics of F-18 Configuration for 0° to 90° Angle of Attack - Test Results and Analysis," NASA Contractor Report 3608, August 1984.

20. Suárez, C.J. and Malcolm, G.N., Dynamic Water Tunnel Tests for Flow Visualization and Force/Moment Measurements on Maneuvering Aircraft", AIAA 95-1843, presented at the AIAA 13th Applied Aerodynamics Conference, San Diego, CA, June 1995.

FIGURES

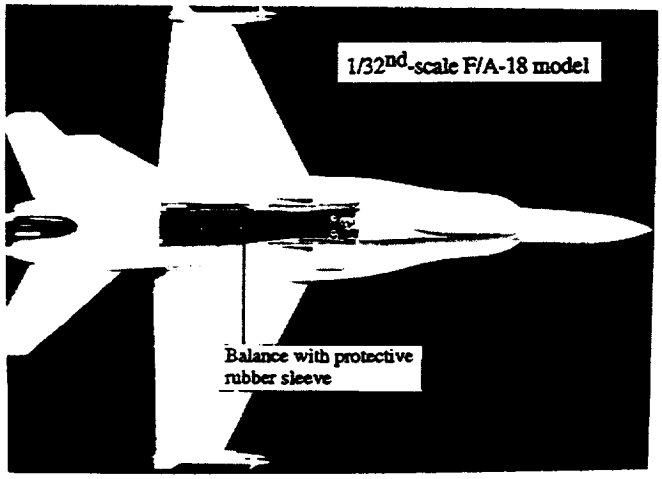

Figure 1 - Water Tunnel Balance Shown in the 1/32nd Scale F/A-18 Model

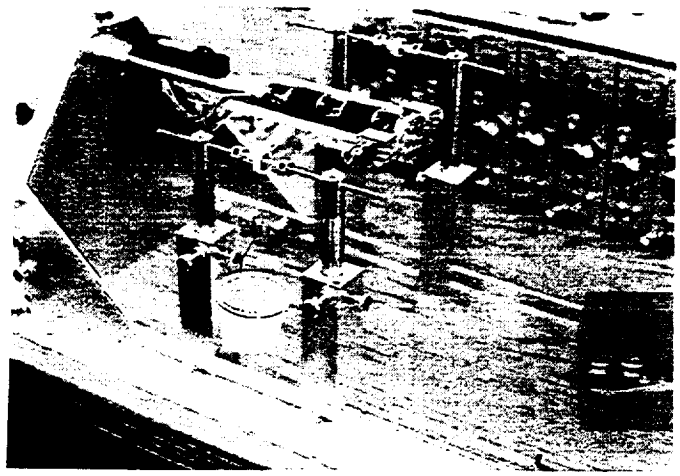

Figure 2 - Calibration Rig

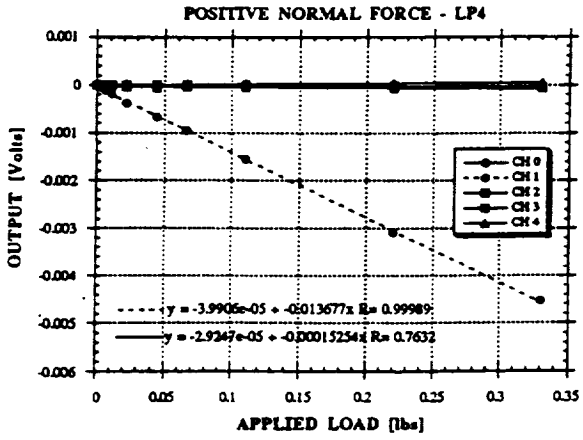

Figure 3 - Balance Response to a Positive Normal Force

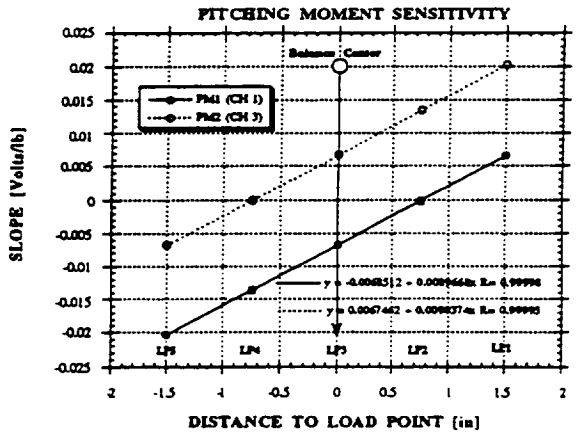

Figure 4 - Pitching Moment Sensitivity

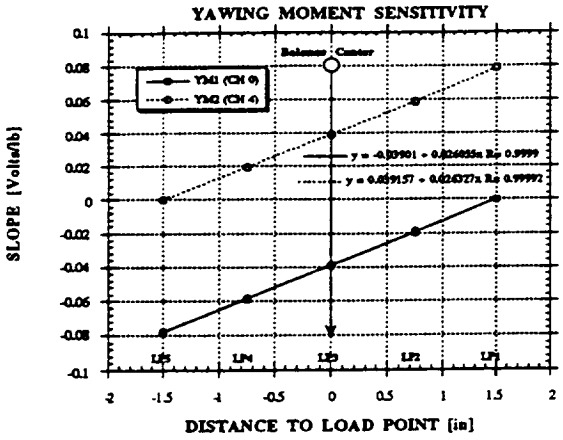

Figure 5 - Yawing Moment Sensitivity

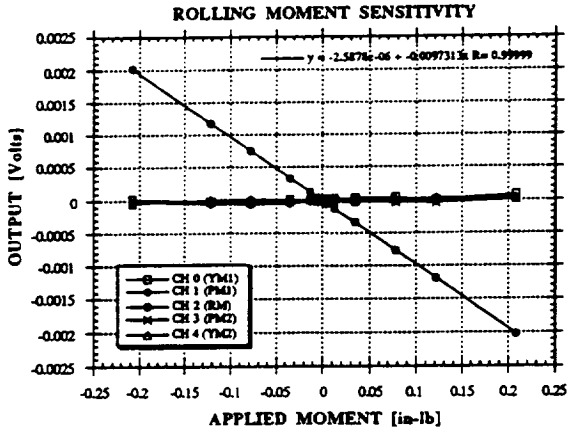

Figure 6 - Rolling Moment Sensitivity

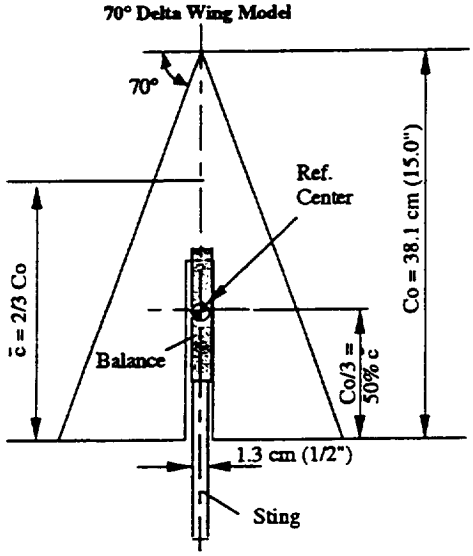

Figure 7 - 70° Delta Wing Model

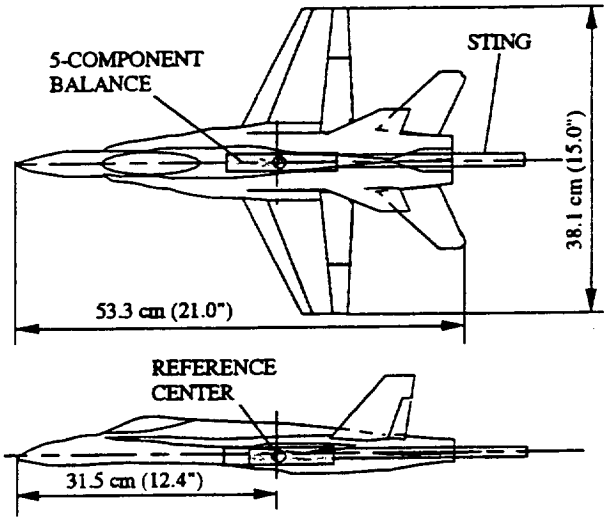

Figure 8 - 1/32nd-Scale F/A-18 Model

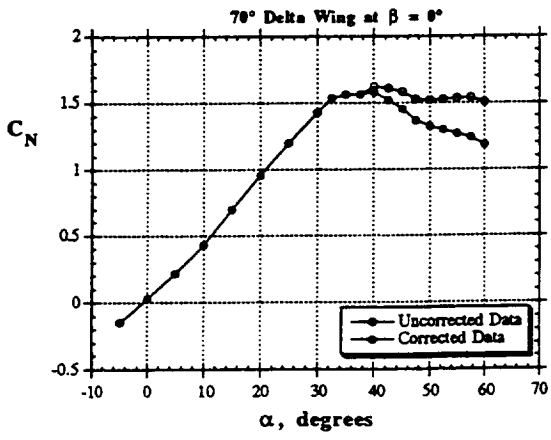

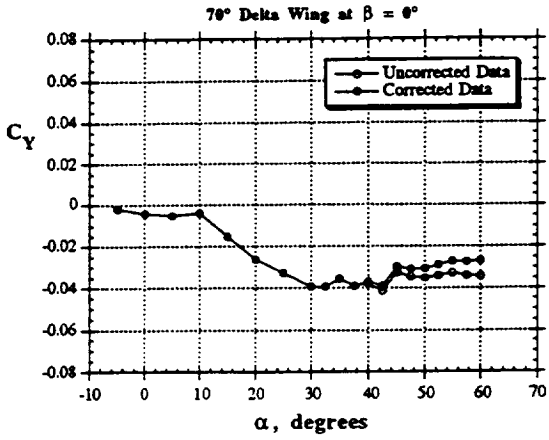

Figure 9 - Effect of Boundary Corrections on Forces (70° Delta Wing)

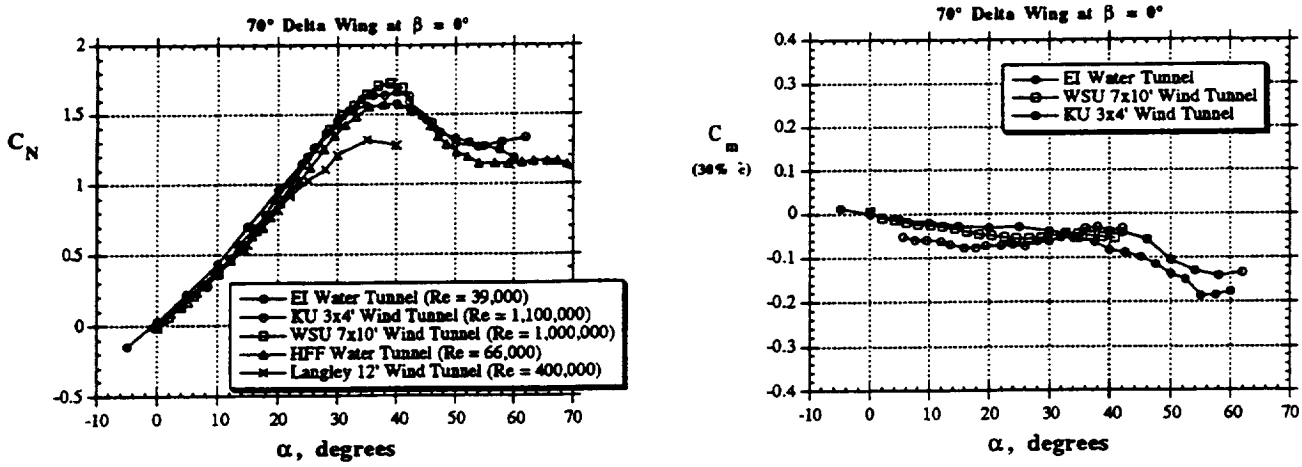

Figure 10 - Longitudinal Characteristics of the 70° Delta Wing

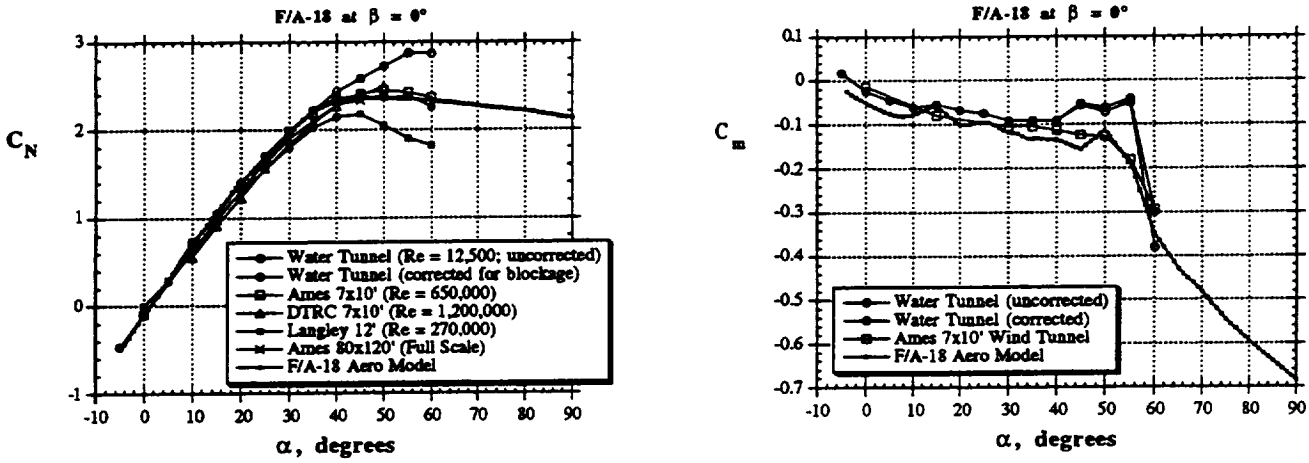

Figure 11 - Longitudinal Characteristics of the F/A-18 Model

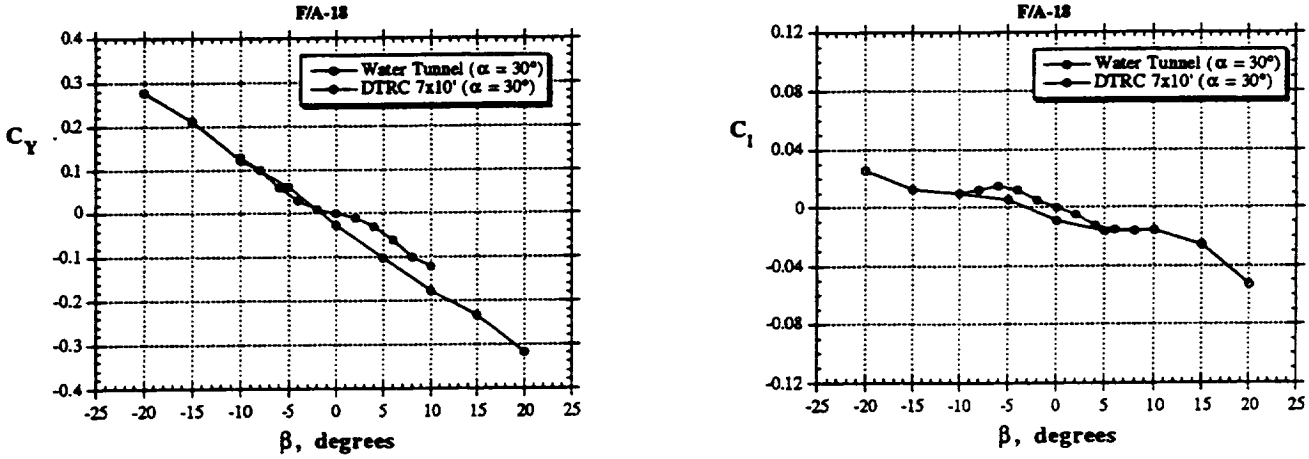

Figure 12 - Lateral/Directional Characteristics of the F/A-18 Model at $\alpha = 30°$

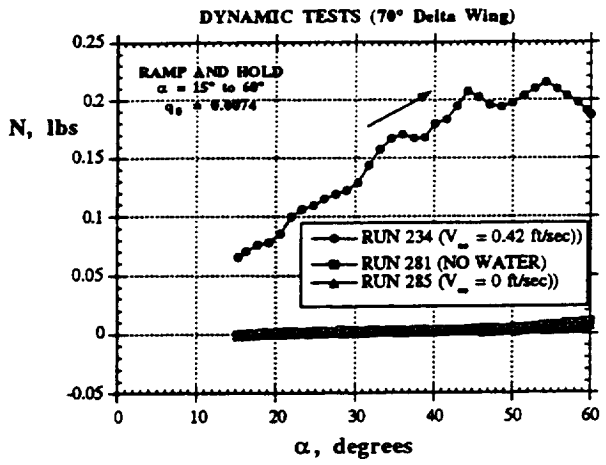

a)

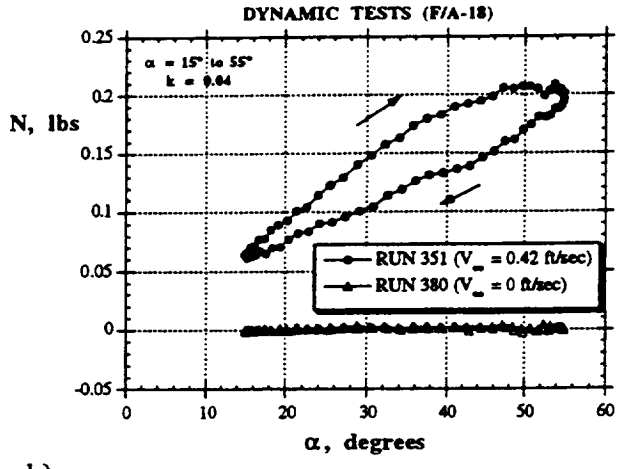

b)

Figure 13 - Inertial Tares During Pitch Maneuvers

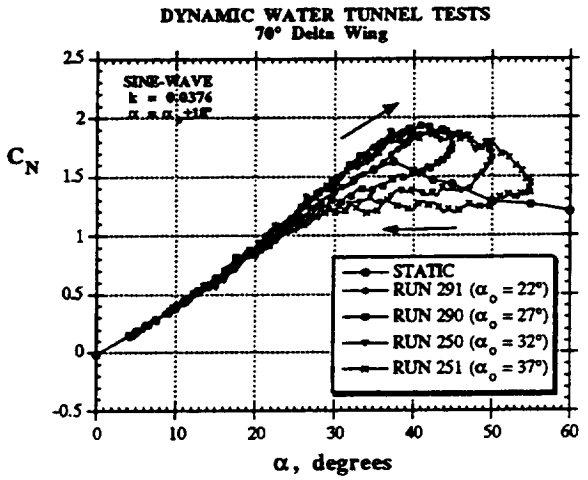

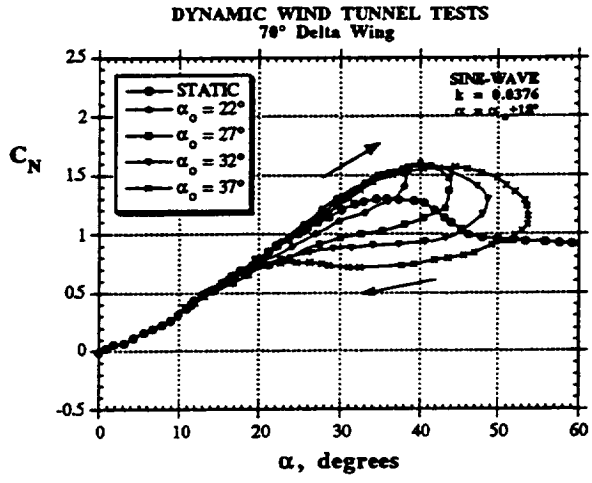

Figure 14 - C_N Variations During Pitch Oscillations about Different Mean Angles of Attack

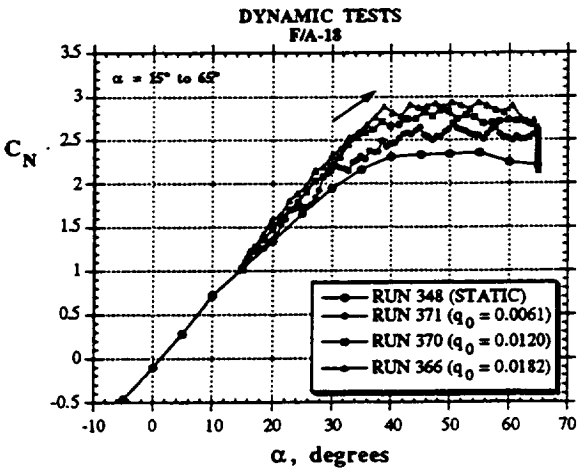

Figure 15 - Pitch-Up and Hold Maneuver

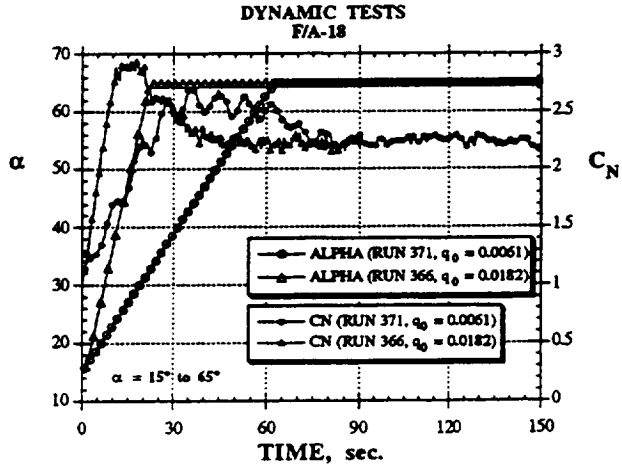

Figure 16 - Pitch-Up and Hold Maneuver

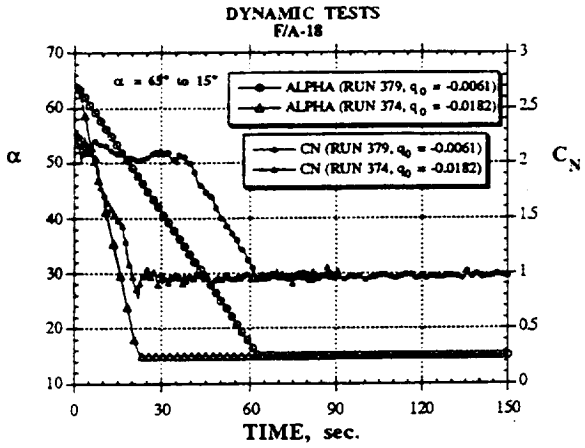

Figure 17 - Pitch-Down and Hold Maneuver

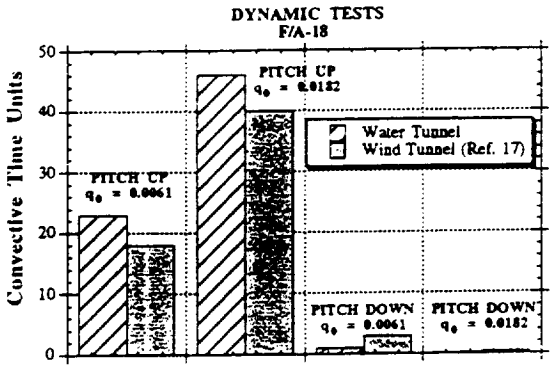

Figure 18 - Persistence of Normal Force

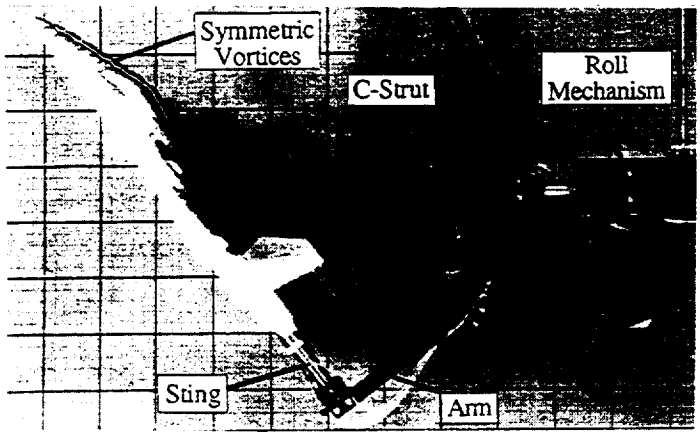

Figure 19 - Rotary-Balance Rig

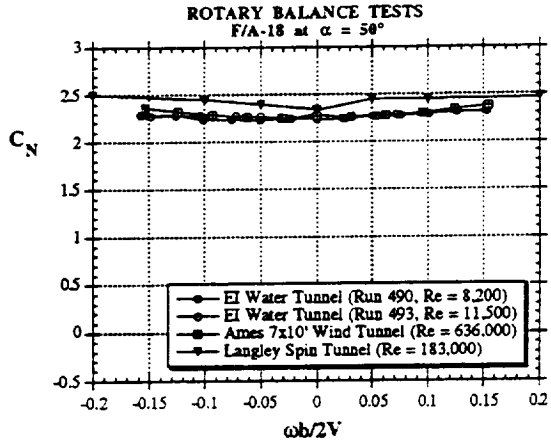

Figure 20 - Rotary-Balance Tests at $\alpha = 50°$

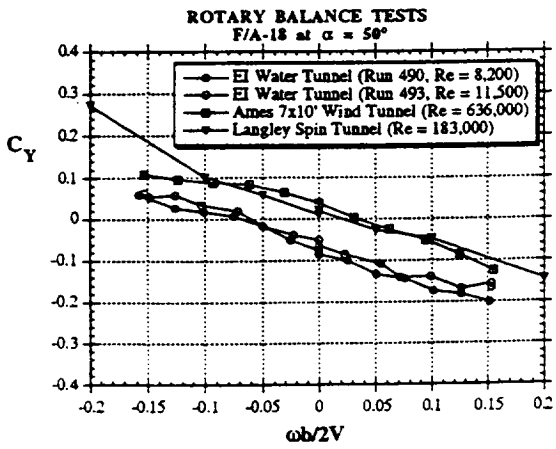

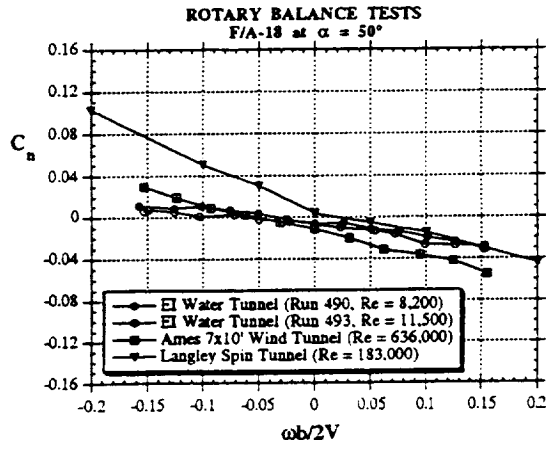

Figure 20 - Continued